

Pyrolysis temperature effect on electrical properties of nanoporous carbon structure derived from olives stones

Wahid djeridi^{#1}, Nabil Ben Mansour², Abdelmottaleb Ouederni¹, Lassaad El Mir^{2,3}

^{#1} *Research Laboratory: Engineering Process et Industrial Systems, National school of Engineers of Gabes, University of Gabes, St Omar Ibn Elkhatab, 6029 Gabes, Tunisia.*
djeridiwahid@yahoo.fr

² *Laboratory of Physics of Materials and Nanomaterials Applied at Environment (LaPhyMNE), Gabes University, Faculty of Sciences in Gabes, Gabes, Tunisia.*

³ *Al Imam Mohammad Ibn Saud Islamic University (IMSIU), College of Sciences, Department of Physics, Riyadh 11623, Saudi Arabia.*

Abstract— Electrical conducting carbon nanoporous structures were explored by changing the pyrolysis temperature of activated carbon prepared by chemical processes from olives stones. The effect of these preparation parameters on the structural and electrical properties of the obtained was studied. The obtained results revealed that, the activated carbon phase was transformed progressively with pyrolysis temperature into carbon conducting phase. The temperature-dependent

conductivity of the activated carbon structures show a semiconducting behaviour.

Keywords— Chemical processes; microporous carbon; pyrolysis; transport properties.

I. INTRODUCTION

Conductive carbon nanocomposites covering a large area in different material applications, is one of the most important subjects in the reason of it's wide range of electrical conductivity that varying within several orders of magnitude, extending from insulators up to conductors. Containing a large surface area, porous carbon structures have been used in a wide variety of applications such as electrodes of supercapacitors, energy storage, gas sensors, advanced catalysts supports, chromatographic packing, and others [1-9]. The electrical properties of carbon materials derived from organic precursors have been studied extensively over the years and have been shown to vary widely depending on the heat treatment temperature (HTT)[10]. Later works [11] described an electron hopping between localized states as the main mechanism for electric conduction for sample treated at 700 °C. The authors have shown that the calculated density of localized states increases with HTT within the range of 600-700 °C. In fact during carbonization, the physical properties, particularly the transport properties, undergo strong modification and depend on texture of the obtained material [12]. This evolution is experimentally related to a loss of heteroatoms, during the pyrolysis [13]. The process of carbonization appears as a solid phase nucleation. In fact, the loss of hydrogen promotes the production of bidimensional

nanolayers [14]. However, although the number of publications on carbons is considerable, no totally satisfactory explanations on the evolution of their electronic properties in the range of carbonization are available. In fact, electrical

properties in carbons depend strongly on structural and textural properties which are very close to the precursor, doping element catalyst and elaboration protocol used.

We present in this paper, a low-cost preparation method of microporous electrical conducting carbon (ECC) structures based lignocelluloses material (olives stones). The analysis of the obtained results revealed that, activated carbon insulating phase was transformed progressively with pyrolysis temperature into ECC phase; this means that the percolation threshold observed in the obtained structure can be defined by thermal treatment process.

II. EXPERIMENTAL

A. Sample preparation

A series of activated carbon pellets were prepared in our laboratory using olive stones in two steps process: chemical activation and carbonization. In the chemical process, some

amount of granular olive stones was mixed with aqueous solution containing 50% H₃PO₄ (w/w) at the weight ratio of 1/3. The suspension of the olive stones in chemical impregnation solution was mixed at 110 °C for 9 hours. Impregnate olive stones powder was used as raw material; with a size of about 80 μm. A mass of 0.6 g of the raw material was placed between the pistons in the dice and the mechanical pressure, P, was loaded on them for 1 min by an oil hydraulic machine. After the compression, the impregnate olive stones ejected from the dice were columnar pellets. The pellets were thermally activated in a fixed bed vertical reactor tubular furnace under nitrogen continuous flow for 3 hours at different carbonization temperatures in the range from 350 °C to 1000 °C. After cooling, activated carbon pellet was washed for several times with hot water until the pH of washing solution became neutral. The samples were dried at 110 °C to get the final product. The nomenclature of each sample includes the pyrolysis temperature and the abbreviation of activated carbon pellets (ACP): for example the activated carbon pellet carbonized at 410 °C will be denoted ACP410.

B. Characterization techniques

The prepared products were characterized using a JEM-200 CX transmission electron microscope (TEM). X-ray diffraction (XRD) patterns of ECC were carried out by a Bruker D5005 diffractometer, using Cu K α radiation ($\lambda=1.5418 \text{ \AA}$). Electrical measurements in a temperature range of 80-300 K were carried out using a liquid nitrogen cryostat where the samples were kept under vacuum during the measurements. Current-voltage measurements were performed using a computer-controlled set up comprising a Keithley 220 current source and an Agilent 34401 A multimeter. For ac measurements an Agilent 4294A impedance analyser was used to collect impedance measurements with a wide frequency range. We employ a parallel mode to measure conductance G using an alternating signal with a voltage amplitude for 50 mV.

III. Results and discussion

Figure 1 exhibits the XRD patterns of the extracted product and after heat treatment at different pyrolysis temperatures (410 °C, 500 °C, 1000 °C) in nitrogen atmosphere. From this figure, it can be outlined that at low pyrolysis temperature materials were amorphous. According to these diffractograms, the samples are partly amorphous as prepared and after pyrolysis, because of the presence of small bands centred at around 26° and 44°, corresponding to (002) and (101) hkl planes, respectively, the most intensive diffraction peaks of graphite phase. The average grain size can be calculated using the Scherrer equation [15].

$$G = \frac{0.9 \lambda}{B \cos \Theta_B} \quad (1)$$

Where λ is the X-ray wavelength Θ_B is the maximum of the Bragg diffraction peak (in radians) and B is the line width at half average value of the crystallites was found about 1 nm. Fig. 2 displays TEM micrograph of ACP500; the sample exhibits significant nanoporous morphology in which pore sizes are about 2 nm in diameter.

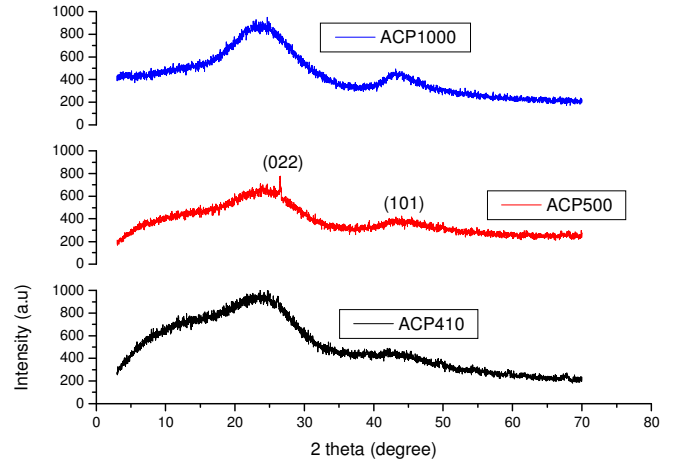


Fig. 1. XRD patterns of: (a) ACP410, (b) ACP500, (c) ACP1000

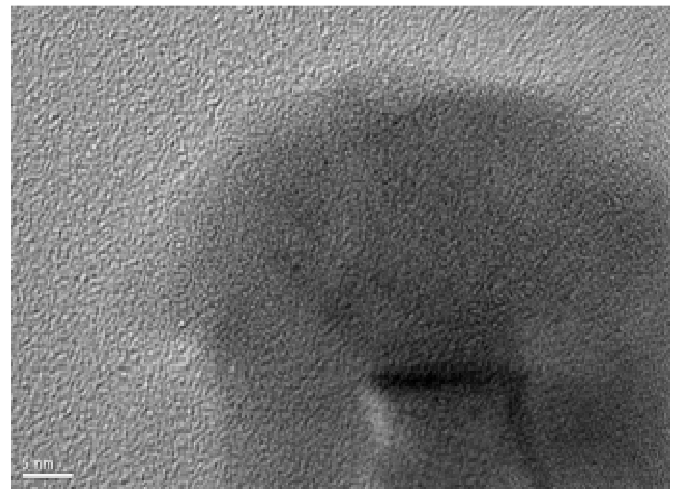


Fig. 2. TEM micrographs of ACP500 sample

The dc room temperature bulk conductivity results as a function of the pyrolysis temperatures are plotted in Figure 3. It is well known that all conductive samples show a characteristic percolation threshold that is dependent on the nature and particle size of the conductor. The DC conductivity change markedly in transition range between 410-600°C. Furthermore, there is a region in the percolation curve where

the conductivity of the samples changes abruptly as the conductor content is increased. This change occurs near the percolation threshold and has the same behavior as illustrated in Figure 3. According to the fact that percolation theory predicts a critical concentration of percolation threshold at which conductive paths are formed in the samples, leading to a conversion from an insulator to a more conductor material [16-20], it is useful to define in our study the percolation threshold by a critical conduction temperature T_c as illustrated in Figure 3. It means that when the porous carbon is heated, the samples can be transformed to electrical conductive particles and the T_c is the pyrolysis temperature corresponding to the beginning of conductive path formation. Figure 3 indicates that the critical conduction temperature for this material resides between 350 and 600°C. In order to determine the critical conduction temperature values, the conductivity versus pyrolysis temperature was fitted to a power law proposed by El Mir et al [21] and given by:

$$\sigma = A(T - T_c)^n, \quad (2)$$

Where σ is the conductivity of the sample, T is the pyrolysis temperature, T_c is the critical conduction temperature, A and n are the fitting constants. The best fit is obtained for $A = 2.24 \cdot 10^{-7} \Omega^{-1} \text{cm}^{-1} \text{K}^{-n}$ and $n = 2.7$ when T_c was assumed to be 410°C. Figure 3 shows that a good fit was achieved between the experimental data (square) and the fit function (triangles). Theoretical predictions of the critical exponent, n , range about 3.1 have been reported [22]. The studies of microporous samples have shown that the electrical characteristics are highly dependent on the pyrolysis temperature and that there is a sample conductivity change of about seven orders of magnitude when the heat treatment temperature is varied between 350°C and 1000°C. This increase may be due in part to the conversion of amorphous carbon into a semi-crystalline phase. The emergence of XRD graphite related bonds for sample pyrolysed at 1000°C, as shown in Figure 1, may consolidate this hypothesis.

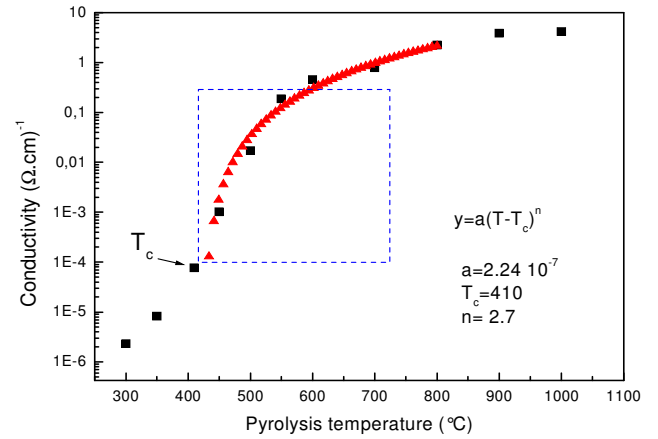


Fig.3. the dc conductivity isotherms versus pyrolysis temperatures

Figure 4 presents the variation of $\ln(G_{dc})$ versus $1000/T$ for ACP500. The curves exhibit activated temperature dependence in accordance with the following equation [23]:

$$G_{dc} = A \exp\left(-\frac{E_a}{k_B T}\right) \quad (3)$$

Where A is the pre-exponential factor including charge carrier mobility and density of states, k_B is the Boltzmann constant, T and E_a are respectively the measurement temperature between 200 and 300 K and the activation energy. The observed linear fits in the high temperature domain, reveals a thermally activated process. The activation energy calculated using equation (3) is the order of 188 meV.

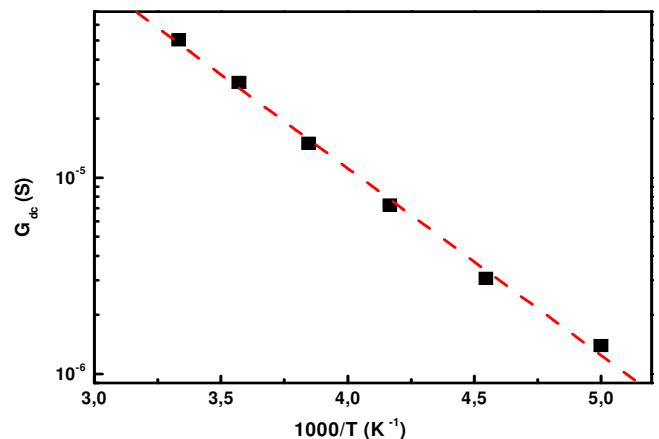


Fig. 4. dc conductance versus $1000/T$ for ACP500 .

Figure 5 shows the frequency dependence of the ac conductance at several measurement temperatures for ACP500. For the full range of frequency, the behavior is semiconductor. In the high frequency domain, the ac sample conductance may follow the Jonscher power law [24]:

$$G(\omega) = G_{dc} + A\omega^s \quad (4)$$

Where G_{dc} is the dc conductance, A is a pre-exponential factor and s is the frequency exponent.

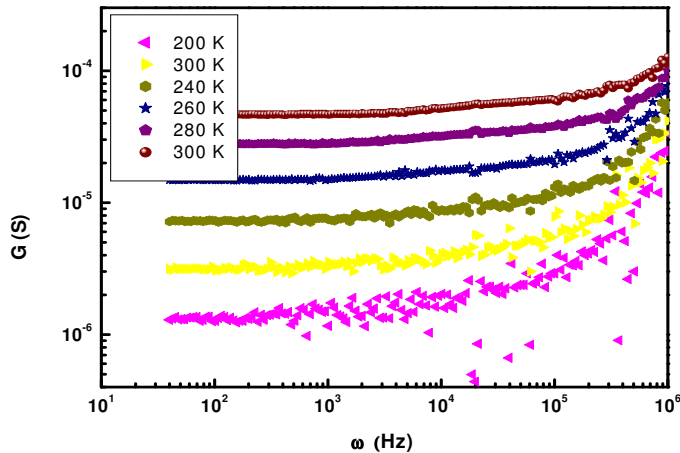


Fig. 5. ac conductance at various measurement temperatures between 200 and 300 K for ACP500

The deduced s values from fits using equation (4), in the high frequency region, for different measurement temperatures indicate that $0 < s < 1$ characterizing the probably dominance of hopping conduction mechanism [25]. The equation (4) is often called “the ac universality law” since it has been found to satisfactorily describe the ac response of numerous different types of materials, which can be classified as disordered solids [26,27], such as ion conducting glasses [28,29], conducting polymers [30] and polymer matrix–conductive filler composites [31].

IV. CONCLUSION

The microporous electrical conducting carbon has been prepared by chemical method combined with a furnace firing in nitrogen atmosphere. The micropore electrical conducting carbon presents some particular behavior. Structural and TEM observations indicates an amorphous nanoporous phase, it has been demonstrated that heat treatment improves the network structure density and increases the carbonization which involve the transformation of the material from insulating into conducting phase.

REFERENCES

- [1] S.T. Mayer, R.W. Pekala, J.L. Kaschmitter, *J. Electrochem. Soc.* 140 (2) (1993) 446.
- [2] G.M. Pajonk, *Appl. Catal.* 72 (1991) 217.
- [3] Y. Hanzawa, K. Kaneko, N. Yoshizawa, R.W. Pekala, M.S. Dresselhaus, *Adsorption* 4 (1998) 187.
- [4] S.H. Joo, S.J. Choi, I. Oh, J.Kwak, Z. Liu, O. Terasaki, R. Ryoo, *Nature* 421 (2001) 169.
- [5] W.C. Choi, S.I. Woo, M.K. Jeon, J.M. Sohn, M.R. Kim, H.J. Jeon, *Adv. Mater.* 17 (2005) 446.
- [6] J. Ding, K.Y. Chan, J. Rena, F. Xiao, *Electrochim. Acta* 50 (2005) 3131.
- [7] F. Su, J. Zeng, X. Bao, Y. Yu, J.Y. Lee, X.S. Zhao, *Chem. Mater.* 17 (2005) 3960.
- [8] F. Lux, *J. Mater. Sci.* 28 (1993) 285.
- [9] M. Carmona, C. Mouney, *J. Mater. Sci.* 27 (1992) 1322.
- [10] J. C. Giuntini, D. Jullien, J. V. Zanchetta, F. Carmona, and A. Delhaes, *J. Non Cryst. Solids* 30, 87 (1978).
- [11] A. Celzard, J. F. Mareche, F. Payot, D. Begin, and G. Furdin, *Carbon* 38, 1207 (2000).
- [12] S. Mrozowski, *Phys. Rev.* 85 (1952) 509.
- [13] N. Job, R. Pirard, J. Marien, J.P. Pirard, *Carbon* 42 (2004) 619.
- [14] J.C. Giuntini, D. Jullien, J.V. Zanchetta, F. Carmona, P. Delhaes, *J. Non-Cryst.Solids* 30 (1978) 87.
- [15] H. Saeki, H. Tabata, T. Kawai, *Solid State Commun.* 120 (2001) 439.
- [16] G.M. Pajonk, *Appl. Catal.* 72 (1991) 217.
- [17] Y. Hanzawa, K. Kaneko, N. Yoshizawa, R.W. Pekala, M.S. Dresselhaus, *Adsorption* 4 (1998) 187.
- [18] S.H. Joo, S.J. Choi, I. Oh, J. Kwak, Z. Liu, O. Terasaki, R. Ryoo, *Nature* 421 (2001) 169.
- [19] W.C. Choi, S.I. Woo, M.K. Jeon, J.M. Sohn, M.R. Kim, H.J. Jeon, *Adv. Mater.* 17 (2005) 446.
- [20] J. Ding, K.Y. Chan, J. Rena, F. Xiao, *Electrochim. Acta* 50 (2005) 3131.
- [21] L. El Mir, S. Kraiem, M. Bengagi, E. Elaloui, A. Ouederni and S. Alaya, *Physica B: Condensed Matter* 395 (2007) 104-110.
- [22] M. Weber, M.R. Kamal, *Polym. Comp.* 18 (6) (1997) 711.
- [23] N.F. Mott, E.A. Davis, *Electronic Processes in Non Crystalline Materials*, Clarendon, Oxford (1979) 157.
- [24] A.K. Jonscher, *Nature* 276 (1977) 673.
- [25] H. Bottger and U.V. Bryskin, *Hopping conduction in solids*. Berlin: Verlag Akademie, (1985).
- [26] J.C. Dyre and T. B. Shroder, *Rev. Modern Phys.*, 72 (2000) 873.

[27] A.K. Jonscher, Universal relaxation law. London: Chelsea Dielectrics Press, (1992).

[28] C.A. Angell, Chem. Rev., 90 (1990) 523.

[29] B. Roling, Solid State Ion, 105 (1998) 185.

[30] M.M. Jastrzebska, S. Jussila and H. Isotalo. J. Mater. Sci., 33 (1998) 4023.

[31] N. Guskos, E. A. Anagnostakis, V. Likodimos, T. Bodziony, J. Typek and M. Maryniak, J. Appl. Phys., 97 (2005) 24304.